

## Excitation Functions and Angular Distributions of Alpha Particles Leading to the Ground and First Excited States of $\text{Be}^7$ in the Reaction $\text{B}^{10}(p,\alpha)\text{Be}^{7*}\dagger$

JAMES W. CRONIN<sup>‡§</sup>

*Department of Physics and Institute for Nuclear Studies, University of Chicago, Chicago, Illinois*

(Received September 28, 1955)

Measurements on the excitation function and angular distribution of  $\text{B}^{10}(p,\alpha)\text{Be}^7, \text{Be}^{7*}$  have been carried out with apparatus which is an improvement over that used for previous measurements. Excitation functions have been measured at laboratory angles of  $90^\circ$  and  $145^\circ$  with respect to the bombarding beam, from 0.8 to 1.65 Mev. Angular distributions have been measured at 1.0, 1.2, 1.36, 1.5, and 1.63 Mev, and at 1.3, 1.5, and 1.63 Mev for the excited state. The excitation functions show resonances at 1.17 and 1.5 Mev for the ground state, and 1.55 Mev for the excited state transition. The resonances are superposed on a continuous isotropic background. The 1.17-Mev resonance shows nearly an

isotropic distribution to the ground state. The 1.5-Mev state shows a distribution which is  $1 - 0.53 \cos^2 \theta$  with very small interference terms. The angular distributions leading to the excited state show a marked asymmetry with the backward angles being favored. The absolute cross section at laboratory  $90^\circ$ ,  $E_p = 1.5$  Mev for the ground state transition, is  $21.1 \pm 4$  mb/sterad. This value is in reasonable agreement with previous work.

The angular distributions are not inconsistent with an assignment of  $3/2^-$  for the 9.70-Mev state and  $7/2^+$  for the 10.06-Mev state in  $\text{C}^{11}$ .

### INTRODUCTION

THE reactions of  $\text{B}^{10}$  with neutrons and protons have always been of interest since they lead to the mirror nuclei of  $\text{Be}^7$  and  $\text{Li}^7$ . These have low-lying first excited states at 434.3 and 479.0 kev, respectively.<sup>1</sup>

The relative yields of  $\alpha$  particles to the ground and first excited states of these nuclei give information concerning the level parameters of the intermediate nuclei  $\text{C}^{11}$  and  $\text{B}^{11}$  and the residual nuclei  $\text{Li}^7$  and  $\text{Be}^7$ . The reactions  $\text{B}^{10}(p,\alpha)\text{Be}^7, \text{Be}^{7*}$  have been studied most extensively by Brown *et al.*,<sup>2</sup> henceforth referred to as BSFL. Figure 1 shows the levels involved in the reactions.

The purpose of this work is to obtain further information on these reactions by measuring the angular distributions of the  $\alpha$  particles, as well as remeasuring

the excitation function and absolute differential cross section.

In the work of BSFL, measurements were hampered by interference of protons scattered from the target. For the present work an apparatus has been constructed to eliminate these background difficulties.

The  $Q$  values for the reactions are low (1.147 and 0.717 Mev)<sup>1</sup> so that for backward angles of observation the energies of the  $\alpha$  particles are lower than the bombarding protons for energies at which the yield is appreciable. In a magnetic spectrograph of the resolving power used in these experiments, the orbits of a doubly charged  $\alpha$  particle and a proton are indistinguishable at the same energy. However, in an electrostatic analyzer, doubly charged alphas are widely separated from protons of equal energy, traversing it at half the field required for the protons. Thus, the use of an electrostatic analyzer is a distinct advantage in this experiment. At a bombarding energy of 0.8 Mev the longer-range  $\alpha$  particle group lies only 70 kev below the region of scattered protons from boron, for a measurement at  $90^\circ$  to the beam. Thus, if thin targets are used to confine the elastically scattered protons in a small energy range, electrostatic measurements can be made relatively free of proton background in an energy range extending from 0.8 Mev upward.

### APPARATUS

The primary objective is to measure the angular distributions of the  $\alpha$  particle groups in the reaction  $\text{B}^{10}(p,\alpha)\text{Be}^7$ . An apparatus has been constructed which has a continuously adjustable angle from  $146^\circ$  in the backward direction to  $14^\circ$  in the forward direction. Figures 2 and 3 show the schematic view of the apparatus. The cylindrical target chamber is designed with a slot halfway around it placed below the line of the beam. A sleeve sealed by "O" rings covers the slot and contains the opening to the cylindrical analyzer. Since the beam line is above the slot, the analyzer must be placed at an angle to the horizontal plane. The true

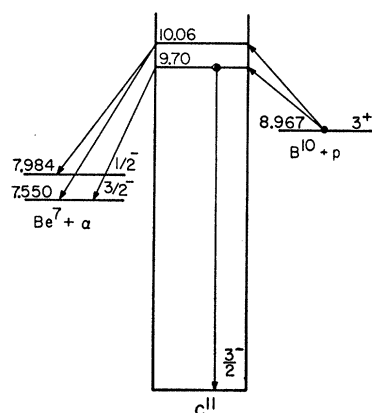


FIG. 1.  $\text{C}^{11}$  energy levels involved in reactions of  $\text{B}^{10}$  plus protons.

\* A thesis presented in partial fulfillment of the requirements for the Ph.D. at the University of Chicago.

† Supported in part by the U. S. Atomic Energy Commission.

‡ National Science Foundation Predoctoral Fellow.

§ Now at Brookhaven National Laboratory, Upton, New York.

<sup>1</sup> F. Ajzenberg and T. Lauritsen, *Revs. Modern Phys.* **27**, 77 (1955).

<sup>2</sup> Brown, Snyder, Fowler, and Lauritsen, *Phys. Rev.* **82**, 159 (1951). This gives a summary of all work previously done on the mirror nuclei  $\text{Be}^7$  and  $\text{Li}^7$ .

angle of the analyzer with respect to the beam is given by  $\cos\theta = \cos\delta \cos\varphi$ , where  $\varphi$  is the projected angle in the horizontal plane and  $\delta$  is the angle of dip from the horizontal plane. A value of  $14.2^\circ$  was chosen for  $\delta$  because it is a good balance between smallness of  $\delta$  and proximity of the analyzer to the target. This arrangement makes possible a continuous change in angle without disturbing the vacuum in the system. Observation windows are provided on the target chamber for aid in alignment and for viewing the condition of the target. On the opposite side from the slot, an "O" ring is placed in a groove flush against the target chamber. When the tube leading to the electrostatic analyzer is adjacent to this "O" ring, the analyzer is sealed off from the target chamber, which can then be filled with air so that targets may be changed without disturbing the vacuum in the analyzer. The system is evacuated with an oil diffusion pump trapped with liquid nitrogen. Vacuums of the order of  $5 \times 10^{-5}$  mm were maintained in the system.

The cylindrical electrostatic analyzer has been used in this laboratory for many years.<sup>3</sup> The analyzer is mounted on a rotating table so that it may turn concentrically with the sleeve which covers the slot on the target chamber. It has a 10-inch average radius, and a plate separation of  $\frac{1}{4}$  inch. The high voltage<sup>4</sup> is measured by the current draining through a precision resistor. For nonrelativistic orbits, the particle energy passed by the analyzer is proportional to the voltage placed across the deflecting plates. If the particle energy is expressed in electron kilovolts and the voltage in kilovolts the constant for this analyzer is  $19.77 \pm 0.11$  for a singly charged ion traversing a median orbit. The analyzer was operated without entrance or exit slits, in which case the solid angle is limited by the walls of the analyzer.

The vacuum line is coupled to the rotating system by a rotating connector concentric with the target chamber and support. The angle of the analyzer with

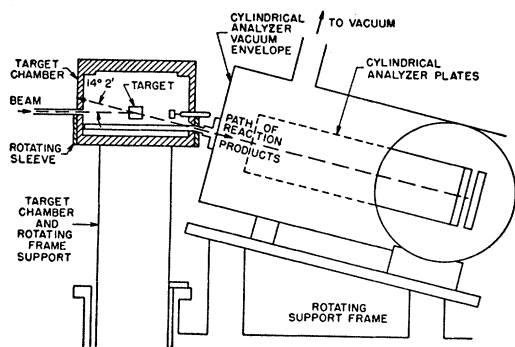


FIG. 2. Side view of experimental apparatus.

<sup>3</sup> Allison, Skaggs, and Smith, Phys. Rev. 54, 171 (1938); P. K. Weyl, Phys. Rev. 91, 289 (1953).

<sup>4</sup> Supplied by 0-50 kv power supply built by Beta Electric Company.

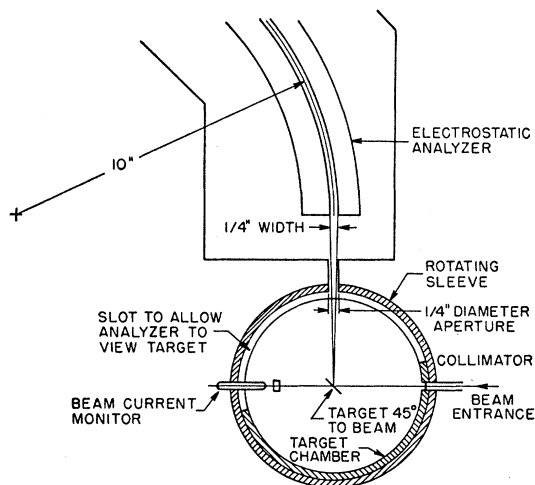


FIG. 3. Top view of experimental apparatus.

respect to the beam is indicated by a scale on the apparatus and is easily read to  $0.5^\circ$ .

The targets are made by evaporating boron 10 on thin nickel films of  $90 \mu\text{g}/\text{cm}^2$  thickness.<sup>5,6</sup>

The detector must satisfy several requirements. Since the reactions have low  $Q$  values, the variation of energy with the angle of observation of the  $\alpha$  particles is very great. Thus, it is important to have a detector which has uniform response over the entire range of  $\alpha$  energies. The detector must be insensitive to small sparks and discharges which occur in the analyzer. A proportional counter was built which satisfied these conditions. The counter is filled with 5 to 6 cm Hg of methane gas, which flows continuously through the counter. The counter is separated from the high vacuum by a pyroxylin foil of about 200-kev stopping power for 1.5-Mev  $\alpha$  particles. The foil is supported by a wire gauze with a 50% transmission.

The proportional counter provides additional discrimination against scattered protons. A 6 cm Hg filling of the counter is such that an  $\alpha$  particle of about 1.2 Mev has a range equal to the depth of the counter chamber. Any proton which can pass through the analyzer for the same voltage setting will have half the energy but still a far greater range, so that the proton pulses are observed to be about  $\frac{1}{4}$  to  $\frac{1}{2}$  the size of the  $\alpha$  pulses. The discrimination between the  $\alpha$  particles and the protons was so effective that no special care was required to have very thin targets. Some of the targets produced scattered protons in a wider energy range than one would expect from their nominal thickness. This caused no difficulty in detecting the lower yield particles because of the effective discrimination.

The source of protons is a 2-Mev Van de Graaff accelerator belonging to the Division of the Biological

<sup>5</sup> Boron obtained from Stable Isotopes Division, Oak Ridge National Laboratory, Oak Ridge, Tennessee.

<sup>6</sup> Films obtained from Chromium Corporation of America, Waterbury, Connecticut.

Sciences, the University of Chicago. This machine has been described by Kahn.<sup>7</sup> The maximum energy spread in the proton beam is 1%.

The beam is collimated by a 0.045 in.  $\times \frac{5}{32}$  in. slit at the entrance to the target chamber. This collimation keeps the beam restricted to a small region on the target which can always be viewed by the analyzer.

The incident proton energy was determined by the energy of the  $\alpha$  groups as measured by the analyzer. The incident energy was then computed by the known  $Q$  values of  $B^{10}(p,\alpha)Be^7$ , 1.147 Mev for the ground state, 0.714 Mev for the excited state.<sup>1</sup>

#### GENERAL PROCEDURE OF MEASUREMENT

The apparatus was first adjusted so that the beam of protons struck the boron target at the center of the reaction chamber. The target was mounted in a slot at the base of the chamber at an angle of 45° with respect to the beam. The analyzer was then adjusted so that it pointed to the center of the chamber for all possible angles of observation. Finally the angular distribution of 0.6-Mev protons scattered from gold was measured. The results were in agreement with the Rutherford scattering formula with no systematic deviation.

The layer of boron on the nickel films was of such thickness that the  $\alpha$  particles were spread in an energy band from 80 to 100 kev wide. This energy spread is too wide for all the  $\alpha$  particles to be accepted for one analyzer setting. Instead of making a measurement at a single point, profiles were taken by varying the voltage on the analyzer and making curves of counts per microcoulomb of beam current plotted against the voltage setting. The information desired from the measurement is the cross section or a number proportional to the cross section.

The data obtained from the profiles are related approximately to the spectrum of  $\alpha$  particles  $f(\epsilon,\theta)d\epsilon d\Omega$  produced at the target by the expression:

$$\left[ \int_0^{\epsilon_{\max}} f(\epsilon,\theta) d\epsilon \right] \Delta\Omega \cong (\Delta\epsilon/\delta\epsilon) \left[ \sum_n Y_n(\theta) \right] / Y_{++}(\bar{\epsilon}),$$

where  $\epsilon$  is the energy of the  $\alpha$  particles,  $\theta$  is the angle of observation,  $\epsilon_{\max}$  is the upper energy limit of the  $\alpha$  particles,  $\Delta\Omega$  is the solid angle subtended by the analyzer,  $\Delta\epsilon$  is the energy separation between each setting of the analyzer in the measurement of a profile,  $\delta\epsilon$  is the width in energy about a mean energy  $\epsilon$  that the analyzer will accept  $\alpha$  particles,  $Y_n(\theta)$  is the yield for the  $n$ th point along the profile, and  $Y_{++}(\bar{\epsilon})$  is the fraction of  $\alpha$  particles that will leave the target in a doubly charged state at an energy  $\bar{\epsilon}$  which is the average energy of the profile. (The profiles are narrow enough that the change in  $Y_{++}(\epsilon)$  over their width is

not important.) The values of  $Y_{++}(\epsilon)$  are obtained from Dissanaika.<sup>8</sup>

The above expression is nearly exact if  $\Delta\epsilon = \delta\epsilon$ . It is a property of an electrostatic analyzer that  $\delta\epsilon$  is proportional to the energy setting  $\epsilon$ , so that  $\delta\epsilon = R\epsilon$ ,  $R$  being the resolution factor of the analyzer.  $R$  is about 2% and  $\Delta\epsilon \cong 8$  kev. For analyzer settings from 1.0 to 1.5 Mev,  $(\Delta\epsilon/\delta\epsilon)$  ranges from 0.40 to 0.26. Errors in the above relation for these values of  $(\Delta\epsilon/\delta\epsilon)$  are shown to be about 1%.

Using the above expression, the cross sections in the center-of-mass system are given by

$$\left( \frac{d\sigma}{d\Omega} \right)_{c.m.} = \left[ \bar{\epsilon} Y_{++}(\bar{\epsilon}) \left( \frac{d\Omega_{c.m.}}{d\Omega_{lab}} \right) \right]^{-1} \times \left[ \sum_n Y_n(\theta)_{c.m.} \right] \left[ \left( \frac{\Delta\epsilon}{\Delta\Omega} \right) R N_t N_p \right],$$

where  $N_t$  is the number of target nuclei/cm<sup>2</sup>, and  $N_p$  is the number of protons which strike the target for each point on the profile.

The conversion to the c.m. system is made by the approximate relations

$$\cos\theta_{c.m.} \cong \cos\theta_{lab} - \alpha \sin^2\theta_{lab} \\ (d\Omega_{c.m.}/d\Omega_{lab}) \cong 1 + 2\alpha \cos\theta_{lab},$$

where  $\alpha$  is a factor containing the masses, bombarding energy and  $Q$  value involved in the reaction. These formulas are given by BSFL.<sup>2</sup> For  $B^{10}(p,\alpha)Be^7$  the expressions are good to 2% or better.

Relative cross sections are obtained by multiplying  $\sum_n Y_n(\theta)$  by the first factor in the above expression (instrument factor).

#### EXCITATION FUNCTIONS

The excitation functions for the ground- and excited-state alpha transitions were measured at 145° and 90° in the lab system. The variation of the center-of-mass angle with energy is quite small, so that the corresponding center-of-mass angles are 151° and 100°, respectively. The excitation functions were obtained by measuring the profiles of the groups as a function of bombarding proton energy. The profiles were measured by the method discussed above. From the profiles  $\sum_n Y_n(\theta)$  was obtained. The corrections were all related to the yield one would expect with a resolution width of the analyzer set for 1.2-Mev alphas. The correction would then be

$$1.2 / \left[ \bar{\epsilon} Y_{++}(\bar{\epsilon}) (d\Omega_{c.m.}/d\Omega_{lab}) \right].$$

The corrections were calculated, and their product with  $\sum_n Y_n(\theta)$  gives the relative yield at the particular angle as a function of bombarding energy. The bombarding energy is measured by the leading edge of the particle

<sup>7</sup> D. Kahn, Phys. Rev. **90**, 503 (1953).

<sup>8</sup> G. A. Dissanaika, Phil. Mag. **44**, 1051 (1953).

group. The two energies are related by:

$$E_\alpha = 0.5433 E_p - 0.730 \text{ Mev for ground-state transition.}$$

$$E_\alpha = 0.5433 E_p - 0.454 \text{ Mev for excited-state transition.}$$

From the relation  $dE_\alpha/dE_p = 0.543$ , an error in the measurement of  $E_\alpha$  makes twice the error in  $E_p$ . The uncertainty in the  $\alpha$  particle measurement is about 1.5%, making the  $E_p$  values uncertain by as much as 3%. For the measurements at  $145^\circ$ , each profile was measured twice, and these two measured values always agreed within statistical accuracy. The excitation function at  $90^\circ$  has each point measured only once. The yields at  $145^\circ$  were such that most points had  $\sum_n Y_n \geq 500$ . At  $90^\circ$ , most points had  $\sum_n Y_n \geq 1000$ . The statistics were limited by the time required to measure an entire profile, which usually consisted of twenty settings of the analyzer. Peak counting rates were of the order of 150/minute.

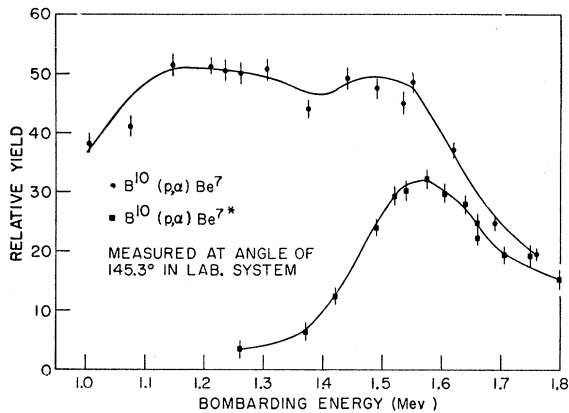


FIG. 4. Excitation functions for the reactions  $B^{10}(p, \alpha)Be^7, Be^{7*}$  at  $145.3^\circ$  in lab system.

Figures 4 and 5 show the results of the excitation function measurements.

The points at  $90^\circ$  in the lab of several of the angular distribution measurements which were made with the same target as the excitation function are plotted as diamonds on the same graph as the excitation function. These points agree quite well with the  $90^\circ$  lab excitation curve. They serve as a check on the reproducibility of the data and as an indication of the stability of the targets. This particular target was used for more than 5000 microcoulombs of proton bombardment. Carbon layers on the target have an effect on the energy determination. Targets were discarded when a visible discoloration appeared and the vacuum system was always trapped with liquid nitrogen. About 3000–5000 microcoulombs of bombardment were required to produce a visible layer. The effect of carbon contamination is believed to be small. A 7-kev layer for  $\alpha$  particles would produce only a 1% error in the energy determination.

#### ANGULAR DISTRIBUTIONS

For a given bombarding energy, the yields are obtained for angles ranging from  $\theta_{lab} = 145^\circ$  to  $\theta_{lab} = 25^\circ$

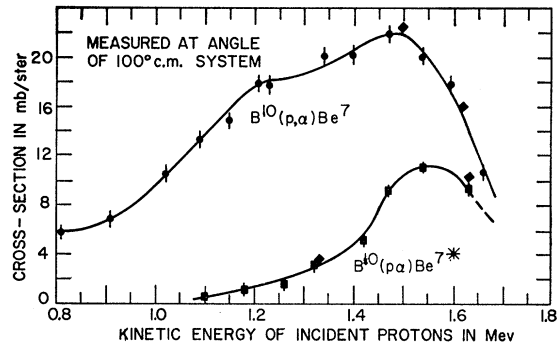


FIG. 5. Cross sections for  $B^{10}(p, \alpha)Be^7, Be^{7*}$  at  $100^\circ$  in the center-of-mass system. The diamond-shaped points are taken from angular distribution measurements made during other runs with the same target. The agreement is evidence of the stability of the target.

in approximately  $10^\circ$  intervals. The collecting efficiency of the analyzer varies strongly with angle because the energy of the  $\alpha$ -particle groups is sensitive to the angle of observation. The backward angles thus have a lower statistical accuracy than the forward ones, since all points are measured for the same number of incident protons.

At higher bombarding energies and at forward angles, the energy of the  $\alpha$  groups is so large that the analyzer will not support sufficient voltage to deflect the groups into the proportional counter. For these cases, low atomic number foils were used to slow the particles down to energies which could be handled by the analyzer. All the measurements using foils were done at forward angles. A calculation of the attenuation of the  $\alpha$  beam by multiple scattering in these foils was performed by a method similar to that of Dickenson

TABLE I. Calculation of corrected yields from raw data for 1.5-Mev angular distribution.

Nominal foil thickness (kev)	Nominal angle (degrees)	cos $\theta_{c.m.}$	b $\sum_n Y_n$	Instrument factor <sup>a</sup>	Corrected <sup>b</sup> yield
				$\frac{1.2}{\bar{\epsilon} Y_{++}(\bar{\epsilon}) d\Omega_{c.m.}/d\Omega_{lab}}$	
0	148°	-0.878	104.5	1.936	202.6
0	140°	-0.822	99.9	1.772	177.0
0	130°	-0.730	139.7	1.560	217.9
0	120°	-0.619	174.2	1.362	237.3
0	110°	-0.487	206.7	1.186	245.1
0	100°	-0.336	250.0	1.038	259.5
0	90°	-0.176	287.8	0.901	259.3
240	90°	-0.176	221.0	1.152	260.0
240	80°	-0.006	254.0	0.964	250.0
240	70°	0.174	295.6	0.822	246.4
500	70°	0.174	221.3	1.081	246.4
500	60°	0.350	265.7	0.933	253.5
500	50°	0.515	302.5	0.794	245.5
500	40°	0.664	293.3	0.704	210.7
500	30°	0.788	316.1	0.630	203.5

<sup>a</sup> Corrected to resolution width at 1.2-Mev  $\alpha$  energy.

<sup>b</sup> A 2% increase is given to the 240-kev foil measurements for normalization. A 3% increase is given to the 500-kev foil measurements.

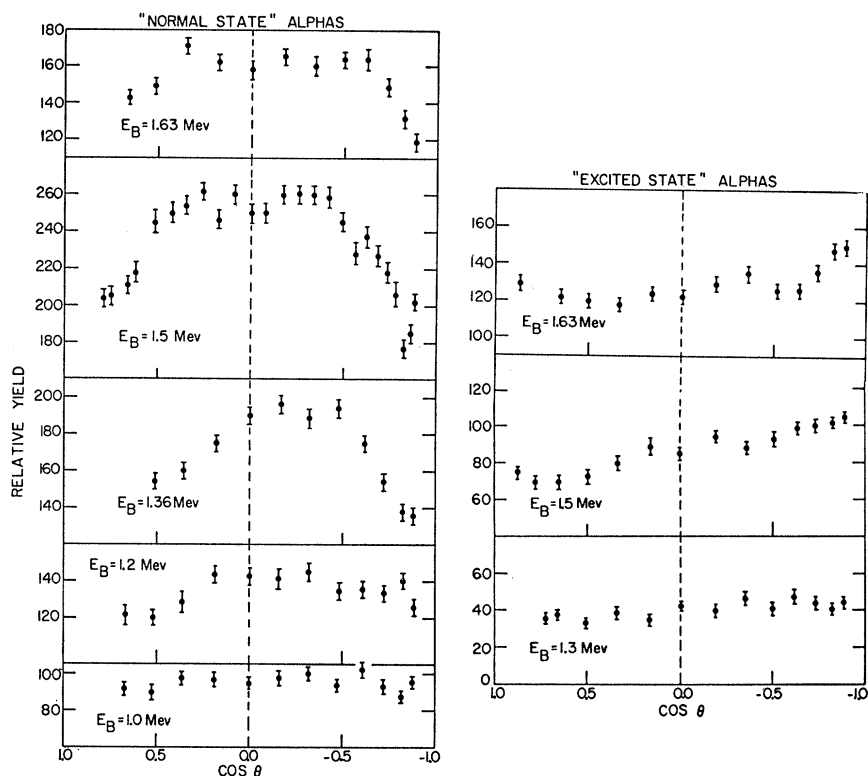


FIG. 6. Experimental results for angular distributions of  $B^{10}(p,\alpha)Be^7, Be^{7*}$ .

and Dodder.<sup>9</sup> The correction for this attenuation proved to be small and was adsorbed in the normalization of the angular distributions for the forward and backward hemispheres at  $90^\circ$  lab.

The backward angle yields were measured with the boron surface of the target facing the beam. The measurements at forward angles were done with the boron facing away from the beam, and having the incident protons traversing the target backing before initiating any reactions. This method allows the maximum angle that the reaction products make with the normal to the target to be  $45^\circ$ . Beyond  $45^\circ$  the path within the target rapidly increases with angle so that straggling and scattering within the target become appreciable and the energy spread of the group becomes wider, so that a longer time is required to measure the profile.

Table I shows how the experimental results are corrected to give the center-of-mass angular distributions for the measurements at 1.5 Mev, for the ground state. For this energy measurements were taken at every  $5^\circ$  because this distribution showed the most marked deviation from isotropy. However, the table only shows the measurements for  $10^\circ$  intervals.

The angular distributions are measured for the ground-state transitions at 1.03, 1.20, 1.36, 1.50, and 1.63 Mev. Excited-state transitions are measured at 1.3, 1.5, and 1.63 Mev. Figure 6 shows the experimental results normalized at  $90^\circ$  lab.

<sup>9</sup> W. C. Dickenson and D. C. Dodder, Rev. Sci. Instr. 24, 428 (1953).

#### ANALYSIS OF ANGULAR DISTRIBUTION INTO EXPANSIONS IN LEGENDRE POLYNOMIALS

The angular distributions are most amenable to theoretical analysis if they are expressed in a series of the form

$$Y(\theta) = Y_0 [1 + \sum_L A_L P_L(\theta)],$$

where  $P_L(\theta)$  are the Legendre polynomials. The analysis into Legendre polynomials follows procedures outlined by Rose.<sup>10</sup>

The angular aperture of the analyzer is  $1^\circ 40'$ . The attenuation coefficients for Legendre polynomials up to the fourth order are shown to be negligible, so that no angular resolution corrections are necessary.<sup>10</sup>

The results were analyzed by the method of least squares to fourth-order Legendre polynomials. This assumes that  $l=2$  is the highest incoming orbital angular momentum contributing to the reaction. In support of this assumption, a calculation was made of ingoing and outgoing penetrabilities. The tables of Coulomb functions of Bloch *et al.* have been used.<sup>11</sup> The channel radius was chosen according to the prescription that  $r_c = 1.4 \times 10^{-13} (A_1^{1/3} + A_2^{1/3})$ . The calculations show that incoming waves with  $l > 2$  can have at most a partial width of one or two kev.

In order to find the least square solution it is necessary to invert a  $5 \times 5$  matrix. These calculations were carried

<sup>10</sup> M. E. Rose, Phys. Rev. 91, 610 (1953).

<sup>11</sup> Bloch, Hull, Broyles, Bouricius, Freeman, and Breit, Revs. Modern Phys. 23, 147 (1951).

TABLE II. Table of coefficients  $A_L$  in the expansion of angular distribution of  $B^{10}(p,\alpha)Be^7, Be^{7*}$  in

$$\text{Series } Y(\theta) = Y_0 \left[ 1 + \sum_1^4 A_L P_L(\cos\theta) \right].$$

Energy (Mev)	$A_1$	$A_2$	$A_3$	$A_4$
		Ground state		
1.03	$0.009 \pm 0.006$	$0.000 \pm 0.004$	$0.075 \pm 0.0020$	$0.043 \pm 0.003$
1.21	$0.026 \pm 0.038$	$0.011 \pm 0.068$	$0.089 \pm 0.051$	$0.157 \pm 0.064$
1.36	$0.072 \pm 0.042$	$-0.100 \pm 0.043$	$0.288 \pm 0.032$	$0.102 \pm 0.027$
1.50	$-0.017 \pm 0.009$	$-0.308 \pm 0.017$	$0.010 \pm 0.017$	$-0.056 \pm 0.022$
1.63	$0.048 \pm 0.037$	$-0.097 \pm 0.060$	$0.092 \pm 0.055$	$0.191 \pm 0.041$
		Excited state		
1.30	$-0.111 \pm 0.041$	$0.000 \pm 0.054$	$0.140 \pm 0.056$	$0.021 \pm 0.060$
1.50	$-0.223 \pm 0.015$	$0.042 \pm 0.024$	$0.000 \pm 0.024$	$0.117 \pm 0.033$
1.63	$-0.127 \pm 0.015$	$0.018 \pm 0.020$	$-0.180 \pm 0.046$	$-0.168 \pm 0.052$

out on the AVIDAC at the Argonne National Laboratory. The yields at each angle were given weights inversely proportional to their statistical error.

Table II shows the values of the coefficients in the expansion in Legendre polynomials. Figure 7 shows the experimental points compared with the least squares fit for the 1.5-Mev ground-state angular distribution.

The higher Legendre polynomials have much of their effect in the regions near  $180^\circ$  and  $0^\circ$ . Since these "ends" of the distributions are not measured, there is no visual proof of their existence in many of the curves. Although the analysis shows such terms (with large errors), their presence does not have the significance of the appearance of the lower order polynomials  $P_1$  and  $P_2$ . The least squares fit and the experimental points for 1.5 Mev agree quite well. The curve passes through the error ranges of  $\frac{2}{3}$  of the points.

#### MEASUREMENT OF THE ABSOLUTE CROSS SECTION

The absolute cross section was measured at 1.5-Mev bombarding energy and  $90^\circ$  in the laboratory system. From our equations relating the yield and the cross section, one must measure the yield from a target of known composition. The measurement is made from a target thick enough to fill the entire energy window of the analyzer. Then the cross section is given in terms of detailed analysis of the reaction. The target is divided into elements of 2-kev thickness for the incoming protons. This defines a number of nuclei/cm<sup>2</sup> for that layer. Then each 2-kev layer contributes  $\alpha$  particles spread over a region in energy, which can be calculated from the stopping power of the  $\alpha$  particles and the kinematics of the reaction. With the energy spread so obtained, one has the yield and cross section related by

$$Y(\epsilon) = N_p N_t (d\sigma/d\Omega) (R\epsilon/\Delta E) \Delta\Omega Y_{++}(\epsilon),$$

where  $\Delta E$  is the spread in energy caused by a 2-kev proton layer and  $N_t$  is the number of target nuclei per cm<sup>2</sup> in a layer 2 kev thick for protons. The target used is a  $B_2O_3$  target containing natural boron, made by evaporating fused  $B_2O_3$  from a tungsten spiral *in vacuo*.

The  $B_2O_3$  evaporates at a little over  $600^\circ C$  so it is assumed that the composition on the target is pure  $B_2O_3$ . Assuming no isotopic fractionation in the evaporation, 18.8% is used as the fraction of  $B^{10}$  in the natural boron to compute the target composition.

Values for the stopping power of  $B_2O_3$  were obtained from work reviewed by Allison and Warshaw.<sup>12</sup> The estimate of the  $\alpha$ -particle stopping powers from the proton data is the largest source of error in the measurement, giving an uncertainty of 15%.

The quantity  $R\Delta\Omega$  is a constant of the analyzer. It was measured by scattering protons from a thick tantalum target and using the same type of analysis as was given above for the  $B_2O_3$  target. Here, the Coulomb cross section can be calculated so that  $R\Delta\Omega$  is the only unknown. The value of the stopping power for tantalum was obtained from the recent measurements on stopping powers of protons in metals by Cooper's group at Ohio State University.<sup>13</sup>

In measuring the yields of protons and  $\alpha$  particles, care was taken to measure the beam current correctly. The collector button was biased positively with respect

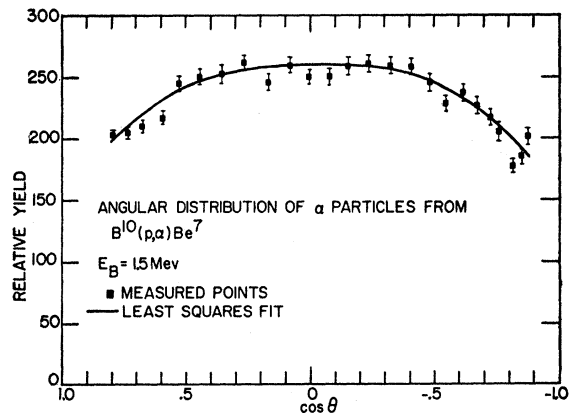


FIG. 7. Least squares fit to experimental data for angular distribution of  $B^{10}(p,\alpha)Be^7$  for bombarding energy of 1.5 Mev.

<sup>12</sup> S. K. Allison and S. D. Warshaw, *Revs. Modern Phys.* **25**, 779 (1953).

<sup>13</sup> Green, Cooper, and Harris, *Phys. Rev.* **98**, 466 (1955).

TABLE III. Calculation of absolute cross section.

Bombarding energy	1.50 Mev $\pm$ 3%
Measured yield $\bar{Y}(\epsilon)$ of ground state alphas from natural $B_2O_3$ target	9.21 counts/ $\mu$ coul $\pm$ 5%
Energy $\epsilon$ of emergent $\alpha$ -particles	1.49 Mev $\pm$ 1%
Stopping power of $B_2O_3$ :	
1.5-Mev alphas	1452 kev/mg $cm^2 \pm 15\%$
1.5-Mev protons	158 kev/mg $cm^2 \pm 7\%$
Fraction $Y_{++}(\epsilon)$ of doubly charged $\alpha$ -particles	0.89 $\pm$ 2%
Energy spread $\Delta E$ of alpha particles from a layer of $B_2O_3$ 2 kev thick for 1.5-Mev protons	19.53 kev
Number $N_t$ of $B^{10}$ nuclei/ $cm^2$ in a 2-kev proton layer of $B_2O_3$	0.412 $\times 10^{17}$
$R\Delta\Omega$	0.251 $\times 10^{-4} \pm 6\%$
Number $N_p$ of protons per $\mu$ coul	6.28 $\times 10^{12}$
$\frac{d\sigma}{d\Omega} = \frac{\Delta E}{N_t \epsilon (R\Delta\Omega) Y_{++}(\epsilon)} \times \frac{\bar{Y}(\epsilon)}{N_p} = 21.1 \pm 4.0$ mb/sterad	

to the chamber to prevent secondary electrons from contributing to the measured current. Table III shows the tabulation of the results and calculation of the cross section.

#### THEORETICAL CALCULATION OF ANGULAR DISTRIBUTIONS

The angular distributions may be calculated theoretically by the equations given in Blatt and Biedenharn,<sup>14</sup> who simplify the formulas by eliminating all sums over magnetic quantum numbers. This procedure introduces "Z" coefficients which are closely related to the Racah coefficients.

A resonant reaction in the simplest case of a single level participating is characterized by quantities  $\alpha s l, J_0, \alpha' s' l'$ . Here  $\alpha$  denotes the particular pair of particles in the ingoing channel,  $s$  is the vector sum of the spins of the pair, and  $l$  is the relative orbital angular momentum between the pair.  $J_0$  is the spin of the compound state through which the reaction passes. The primed quantities have identical definitions for the outgoing channels. For the case, in which only these quantities enter into the reaction, the differential reaction cross section is:

$$\frac{d\sigma}{d\Omega}(\alpha s l, J_0, \alpha' s' l') = \frac{\lambda_{\alpha}^2}{2s+1} \sum_{L=0}^{\infty} B_L P_L(\cos\theta),$$

where

$$B_L = \frac{(-1)^{s'-s}}{4[(E-E_0)^2 + (\frac{1}{2}\Gamma)^2]} [g_{\alpha s l}]^2 [g_{\alpha' s' l'}]^2 \times X(lJ_0lJ_0; sL) Y(l'J_0l'J_0; s'L).$$

$E_0$  is the resonant energy,  $\Gamma$  is the total width, and  $g_{\alpha s l}$  is the square root of the partial width  $\Gamma_{\alpha s l}$ , and represents the amplitude for the participation of a partial wave  $l$  in the reaction. The  $g_{\alpha s l}$  are proportional

<sup>14</sup> J. M. Blatt and L. C. Biedenharn, Revs. Modern Phys. 24, 258 (1952).

to the square root of the penetrability,  $1/(F_l^2 + G_l^2)$ . In terms of our notation in the expansion of the angular distribution into  $(1 + \sum l^4 A_L P_L)$ ,  $A_L = B_L/B_0$ .

The Z coefficients are defined by Biedenharn, Blatt, and Rose.<sup>15</sup> The most useful tabulation of the Z coefficients for this problem is given by Sharp *et al.*<sup>16</sup>

The angular distributions cannot be uniquely calculated with the above expression because the mixing of several channel spins may be possible and the mixing of small amounts of higher  $l$  values may greatly change the angular distribution.

In this specific reaction, the nucleus  $B^{10}$  has  $I=3^+$ , and the proton has  $I=\frac{1}{2}^+$ , so one may have channel spins of  $7/2$  and  $5/2$ . In the outgoing channels,  $Be^7$  has spin  $3/2^-$  and  $1/2^-$  for the ground and excited states, respectively, and  $\alpha$  has spin 0 so that there is a unique channel spin. The outgoing channel for the excited state is further simplified by the spin of  $1/2^-$ . Only one value of  $l'$  is allowed which conserves both parity and angular momentum in the outgoing channel.

In general, one would expect that the major contribution to the angular distribution for a given  $J_0$  would come from the lowest possible  $l$  value if more than one is allowed, but a small admixture of a higher  $l$  value may change the angular distribution significantly. If  $l$  is the lowest possible value, then  $l+2$  is the next possible value in order to conserve parity. If one defines a  $\delta = g_{\alpha s(l+2)} / (|g_{\alpha s(l+2)}| + |g_{\alpha s l}|)$ , one may calculate the angular distribution coefficients as a function of  $\delta$ . This procedure is the same as that used by Stelson.<sup>17</sup>

If mixing of  $l$  occurs only in the incoming channel, the coefficients of the angular distribution are given by,

$$B_L = [Z\{lJ_0lJ_0; s l\} (1 - |\delta|)^2 + Z\{lJ_0(l+2), J_0; sL\} 2\delta(1 - |\delta|) \cos(\xi_{l+2} - \xi_l) + Z\{(l+2), J_0(l+2), J_0; sL\} \delta^2] [Z\{l'J_0l'J_0; s'L\}].$$

Here  $\xi_{l+2} - \xi_l$  is the phase difference between the two partial waves and is given by

$$\xi_{l+2} - \xi_l = \left[ \tan^{-1}\left(\frac{\eta}{l+2}\right) + \tan^{-1}\left(\frac{\eta}{l+1}\right) \right] - \left[ \tan^{-1}\left(\frac{F_{l+2}}{G_{l+2}}\right) - \tan^{-1}\left(\frac{F_l}{G_l}\right) \right],$$

where  $\eta = Z_1 Z_2 e^2 / \hbar v$  and  $F_l$  and  $G_l$  are the regular Coulomb functions evaluated at the nuclear radius. This analysis will be used in the discussion.<sup>18</sup>

#### RESULTS

The general features of the excitation curves agree with those of BSFL. Our measurements can be inter-

<sup>15</sup> Biedenharn, Blatt, and Rose, Revs. Modern Phys. 24, 249 (1952).

<sup>16</sup> Sharp, Kennedy, Sears, and Hoyle, Chalk River Report CRT-556, 1954 (unpublished).

<sup>17</sup> P. H. Stelson, Phys. Rev. 96, 1564 (1954).

<sup>18</sup> Note that the modification of the angular distribution goes as  $\delta$ , while the complexity (i.e., appearance of higher order Legendre polynomials) goes as  $\delta^2$ .

preted in terms of resonances at 1.17 and 1.5 Mev, corrected for barrier, superimposed on a broad continuous background. BSFL find resonances at 1.0 and 1.5 Mev.

Our excitation curve at 151° c.m. may be compared to BSFL at 143° c.m. Their curve is lower at the second resonance whereas ours shows the two resonances to be of about equal intensity. BSFL mention that their data may be low at higher bombarding energies.

The resonances leading to the excited state of Be<sup>7</sup> is centered at 1.55 Mev. It is superimposed on a background that is increasing with energy. There seems to be a consistent effect that the resonance for the excited state transition has its peak at a slightly higher energy than the ground-state peak. The excitation curve of BSFL seems to show the same effect. The rising background may account for part of this apparent shift. Measurements beyond the resonance show that the cross section does not drop off as rapidly as it rises, indicating other contributions to the reaction. The location of the levels correspond to levels at 9.70 and 10.06 Mev in C<sup>11</sup> as given by Ajzenberg and Lauritsen.<sup>1</sup>

The absolute cross sections are in agreement with BSFL within experimental error. Table IV gives a comparison of the cross sections. The BSFL cross sections are corrected to 90°<sub>lab</sub> (100°<sub>c.m.</sub>) by the angular distributions measured in this work.

The angular distributions are flat in the region of 90° c.m. so that the excitation curves at 90° c.m. and 100° c.m. are much alike. At 90° c.m., all odd-order interference terms are zero, so that the excitation curve shows the same shape as the total cross-section curves where the contributions of the two resonances add without interference.

The total widths obtained from the excitation curves are estimated to be  $\Gamma=300$  kev for the lower energy resonance, and  $\Gamma=250$  kev for the higher energy resonance. The resonance for the excited-state reaction has about the same width as the ground-state resonance. Lack of separation of the two resonance peaks makes an estimate of the error in the widths difficult.

The angular distribution measurements show the first resonance (denoted I) and the background to be isotropic. The second resonance (denoted II) shows a marked  $\cos^2\theta$  term. Figure 8 shows a plot of the coefficients of the Legendre polynomials as a function of bombarding energy. The errors for the coefficients have been stated in Table II. The most striking feature of these curves is the sharp peak of the odd order co-

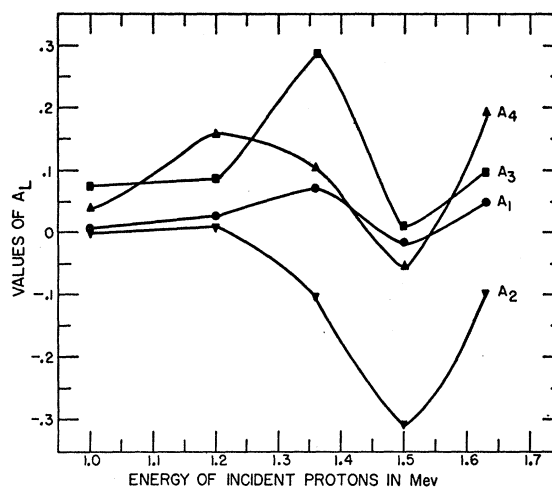


FIG. 8. Variation of values  $A_L$  in the expansion of the angular distribution in a series  $Y(\theta) = Y_0[1 + \sum A_L P_L(\theta)]$  with proton bombarding energy.

efficient in the region directly between the two resonances. This indicates that the two levels must have opposite parity.

The angular distributions enable one to calculate the total cross sections for the reaction. These are  $4\pi \times 17 \times 10^{-27}$  cm<sup>2</sup> and  $4\pi \times 18.4 \times 10^{-27}$  cm<sup>2</sup> at 1.2- and 1.5-Mev proton bombarding energy, respectively. The background appears isotropic and uniform in the region of the resonances with a total cross section of  $4\pi \times 6 \times 10^{-27}$  cm<sup>2</sup>. Subtracting off this amount gives  $4\pi \times 11 \times 10^{-27}$  cm<sup>2</sup> and  $4\pi \times 12.4 \times 10^{-27}$  cm<sup>2</sup> for the total cross sections for resonances I and II, respectively.

The calculation of the total cross section of the resonant reaction to the excited state of Be<sup>7</sup> is made uncertain by the presence of nonresonant background, which increases with bombarding energy. Since asymmetry at about 90° c.m. occurs, one assumes that at 90° c.m. the excitation function is free of interference terms, and that the background may be subtracted off. The background is estimated from the rise in excitation function beyond the resonance. The total cross section for the resonant part of the reaction is  $4\pi \times 7.8 \times 10^{-27}$  cm<sup>2</sup> on the basis of these assumptions. The total resonant cross sections are felt to be correct within  $\pm 20\%$ .

#### DISCUSSION AND INTERPRETATION OF RESULTS

Lower limits on the  $J$  value of the compound state may be imposed by a knowledge of the absolute cross section. The total cross section for a resonant reaction at the peak may be written as

$$\sigma_t = \frac{2J+1}{(2s+1)(2I+1)} \frac{4\pi\lambda^2}{(\Gamma_p + \Gamma_r)^2} \Gamma_p \Gamma_r$$

where  $\Gamma_p$  is the partial width for the incoming channel,  $\Gamma_r$  is the partial width for reactions leading to all other

TABLE IV. Comparison of differential cross section for B<sup>10</sup>(p, $\alpha$ ) at 100°<sub>c.m.</sub> measured in this work with those given in BSFL.

Energy (Mev)	Transition	BSFL mb/sterad	This work mb/sterad
1.2	Ground	16	17.3 $\pm$ 3.5
1.5	Ground	17	21.1 $\pm$ 4.0
1.5	Excited	9.6	10 $\pm$ 2.0



TABLE V. Comparison of reduced widths of resonance I with Wigner sum rule limit.

Channels	Solution 1		Solution 2	
	$\Gamma_s$ (keV)	$\frac{2}{3} \frac{\gamma_s^2 MR_s}{\hbar^2}$	$\Gamma_s$ (keV)	$\frac{2}{3} \frac{\gamma_s^2 MR_s}{\hbar^2}$
$\alpha$	225	8%	75	2.7%
$p$	75	0.8%	225	2.5%

channels,  $I$  is the target nucleus spin, and  $s$  is the projectile spin. The maximum value that the expression  $\Gamma_p \Gamma_r / (\Gamma_p + \Gamma_r)^2$  has is  $\frac{1}{4}$  when  $\Gamma_p = \Gamma_r$ , so that one has the inequality

$$\sigma_t \leq \pi \lambda^2 \frac{2J+1}{(2s+1)(2I+1)}$$

Resonance I has its only reaction channel to the ground state of  $\text{Be}^7$ , with a total cross section of  $4\pi(11.0 \pm 2.2) \times 10^{-27} \text{ cm}^2$ . Resonance II has its reaction channels to either the ground or first excited states of  $\text{Be}^7$ , if we assume that the same resonance level is contributing to the two modes of decay. (Making the assumption of distinct resonances leads to immediate difficulty.) The total reaction cross section for II is then  $4\pi \times [20.2 \pm 4.0] \times 10^{-27} \text{ cm}^2$ . Limits on  $J$  are then given by

$$\text{I: } 2J+1 \geq 3.08 \pm 0.6, \quad J_{\min} = 3/2;$$

$$\text{II: } 2J+1 \geq 7.0 \pm 1.4, \quad J_{\min} = 5/2.$$

The angular distribution for resonance I is nearly isotropic. (The anisotropy is thought to be due to interference terms between the two resonances.)  $3/2^-$ ,  $5/2^+$ , and  $7/2^+$  give isotropic distributions and at the same time satisfy the  $J \geq 3/2$  condition. Spins  $7/2^+$  and  $5/2^+$  may be formed by  $l=0$  and channel spins  $7/2$  and  $5/2$ , respectively, in the entrance channel which yields immediately an isotropic distribution. Spin  $3/2^-$  formed by  $l=1$  waves may decay to the  $3/2^-$  ground state of  $\text{Be}^7$  by  $l'=0$ , yielding an isotropic angular distribution. Of these choices, we discard  $7/2^+$  on the basis that  $l'=3$  is required for  $\alpha$  decay to either the ground or first excited state of  $\text{Be}^7$ . This assignment would allow one to expect some yield to the excited state, which is not observed.  $3/2^-$  is chosen over  $5/2^+$  by appealing to evidence obtained in measurements on the mirror nucleus  $\text{B}^{11}$  by Li and Sherr.<sup>19</sup> They study levels which appear at 9.86 Mev and 10.23 Mev in  $\text{B}^{11}$  by inelastic scattering of  $\alpha$  particles on  $\text{Li}^7$ . By means of analysis by Wigner sum rule limits they place an upper bound for the angular momentum of these levels. For the lower energy resonance,  $J \leq 3/2^+$  or  $J \leq 5/2^-$ . If these levels are really mirror levels to  $\text{C}^{11}$ , then  $3/2^-$  is the favored value for the angular momentum.

Since the absolute cross section and total width of the level is known, the partial widths may be calculated and the results compared with Wigner sum rule limit.<sup>20</sup>

<sup>19</sup> C. W. Li and R. Sherr, Phys. Rev. **96**, 389 (1954).

<sup>20</sup> T. Teichman and E. P. Wigner, Phys. Rev. **87**, 123 (1952).

The reduced widths are calculated with the aid of the barrier penetrabilities given above. The total width of the level is  $\Gamma=300$  keV. The equation for the partial width is quadratic, which gives two solutions (Table V).

The  $3/2^-$  assignment is consistent with the results of measurements on  $\text{B}^{10}(p,\gamma)\text{C}^{11}$  by Day and Huus.<sup>21</sup> They find a resonance at 1.2 Mev for  $\gamma$  decays to the ground state.

Comparing the absolute cross section for  $\gamma$  decay and the cross section for  $\alpha$  decay gives an estimate of the width of about 10 ev. The transition  $3/2^-$  to  $3/2^-$  is a magnetic dipole. The magnetic dipole transition estimate<sup>22</sup> is  $\Gamma_\gamma = 18$  ev.

The angular distributions show a very strong odd order interference between the two levels so that the two must have opposite parities. This restricts the angular momentum to  $5/2^+$ ,  $7/2^+$ , and  $9/2^+$  for resonance II. The spin of II must be such as to allow an appreciable yield to the excited state of  $\text{Be}^7$ . Of these, only  $7/2^+$  gives equal  $l'$  values of 3 for  $\alpha$  decay to either state. Though  $l'=3$  is large, the penetrabilities are relatively insensitive to  $l'$ .

$7/2^+$  may be formed by  $l=0$  waves with channel spin equal to  $7/2$  or by  $l=2$  with channel spin equal to  $7/2$

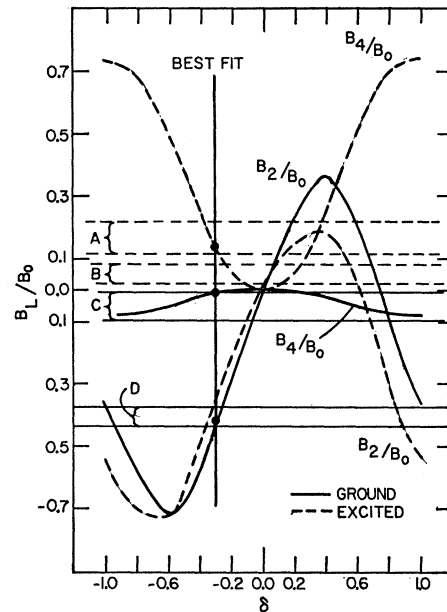


FIG. 9. Calculated variation of the coefficients  $B_L/B_0$  in the angular distribution for resonance II as a function of the mixing parameter  $\delta = g_2 / (|g_2| + |g_0|)$  for channel spin  $7/2$  and  $J=7/2^+$ . The horizontal bars across the graph are the experimentally measured values for the coefficients  $B_L/B_0$ . The width of the bars gives the limit of error. A and B are the experimental values of  $B_4/B_0$  and  $B_2/B_0$ , respectively, for the excited-state transition. C and D are the experimental values for  $B_4/B_0$  and  $B_2/B_0$ , respectively, for the ground-state transition. The vertical line represents the best fit for  $\delta = -0.3$ .

<sup>21</sup> R. B. Day and T. Huus, Phys. Rev. **95**, 1003 (1954).

<sup>22</sup> J. M. Blatt and V. F. Weisskopf, *Theoretical Nuclear Physics* (John Wiley and Sons, Inc. New York, 1952), p. 627.

or  $5/2$ . The angular distribution is very sensitive to admixtures of  $l=2$ . The angular distribution due to the resonance is obtained by subtracting off the isotropic background from the measured distribution. This gives a distribution of  $1-0.414P_2(\theta)$ . This can be fitted by an admixture  $\delta=g_2/(|g_2|+|g_0|)=-0.3$  of  $l=2$  waves. Figure 9 shows how the angular distributions vary with the mixing parameter  $\delta$ . The bars across the graph express the measured coefficients with their errors.

The angular distribution due to the excited state resonance is obtained by neglecting the odd-order interference terms, and subtracting from the total intensity an amount which is obtained by estimating the nonresonance intensity at the  $100^\circ$  c.m. measurement. The corrected distribution is given by,  $Y(\theta) \cong 1+0.06P_2+0.167P_4$ . This distribution seems not completely consistent with the ground state distribution. In Fig. 9, the  $P_4$  term does agree, while the  $P_2$  term does not. An argument may be made that the distributions are not inconsistent. Since the interference between the resonance and the background shows a strong  $P_1$  term, this must be interference from an odd-parity state. This would require  $l=1$  waves in the entrance channel.  $l=1$  may have an angular distribution which is as complex as  $P_2(\theta)$ . Thus one would not expect the  $P_2(\theta)$  term to agree with the distribution calculated for the single resonance, because the background itself may contribute to  $P_2(\theta)$ . The  $P_4(\theta)$  term should be consistent within the uncertainty of subtracting off the background. This agreement is actually achieved as Fig. 9 shows. The failure<sup>22</sup> of the appearance of a  $\gamma$ -ray resonance to the ground state of  $C^{11}$  is also additional support for the  $7/2^+$  assignment, which would be a magnetic quadrupole transition. On the assumption of  $J=7/2^+$  and  $\Gamma=250$  kev obtained from the excitation functions, the reduced widths for the resonance II may be compared with the Wigner sum rule limits. The branching ratio  $\Gamma_\alpha/\Gamma_{\alpha'}$  (prime indicating the excited state transition) is obtained from the ratio of the total cross sections. The two solutions are given in Table VI. Of the two solutions, solution (1)

TABLE VI. Comparison of reduced widths of resonance II with Wigner sum rule limit.

Channels	Solution 1		Solution 2	
	$\Gamma_s(\text{kev})$	$\frac{2}{3} \frac{\gamma_s^2 MR_s}{\hbar^2}$	$\Gamma_s(\text{kev})$	$\frac{2}{3} \frac{\gamma_s^2 MR_s}{\hbar^2}$
$P$	160	13%	90	9%
$\alpha$	56	15.7%	100	32%
$\alpha'$	34	20.3%	60	42%

is preferable, since it does not give such large percentages of the Wigner limits.

The data are sufficient to establish that  $J_I \geq 3/2$ ,  $J_{II} \geq 5/2$ . Detailed analysis of the data strongly suggests spin and parity assignments of  $3/2^-$  and  $7/2^+$  for the levels at 9.70 and 10.06 Mev in the level scheme of  $C^{11}$ .<sup>23</sup> All evidence here is consistent with the assumptions of  $3/2^-$ ,  $1/2^-$  for the ground and first excited states of  $Be^7$ , respectively. The data are consistent with other work on related reactions.

#### ACKNOWLEDGMENTS

The author would like to express his thanks to Professor Samuel K. Allison, under whose sponsorship this work was performed, for all his advice, assistance and encouragement, and for extending the full facilities of his laboratory. The author extends appreciation to Dr. William Bloom and Dr. Raymond Zirkle of the Committee of Radiobiology and Biophysics for the use of the accelerator, and their fullest co-operation. Special thanks are due to Sam Iwaoka, engineer to the Van de Graaff, for helping keep the machine in good running order. A discussion with Dr. J. A. Simpson concerning the construction of a proportional counter greatly facilitated the work. The author is indebted to Professor H. L. Anderson for discussion about least squares analysis with the AVIDAC, and to Dr. W. C. Davidon who assisted with the analysis.

<sup>23</sup> Disregarding the evidence from the mirror nucleus  $B^{11}$ , one might consider assignments of  $5/2^+$ ,  $5/2^-$  for the resonances I and II, respectively. This assumption leads to disagreement with the observed angular distributions.